

$$\hat{\psi}_{2\alpha\beta} = \frac{\hat{M}}{1 + (p - j\omega_m)\tau_2} \cdot i_{1\alpha\beta} \quad (1)$$

$$i_{1dq}^* = i_{1d}^* + j i_{1q}^* = G_{AFR} \left(|\psi_2|^* - |\psi_2| \right) + j \frac{T^*}{|\psi_2|^*} \quad (2)$$

$$i_{1dq} = \frac{\hat{\psi}_{2\alpha\beta}}{|\hat{\psi}_2|} i_{1\alpha\beta} \quad (3)$$

$$v_{1\alpha\beta}^* = \frac{\hat{\psi}_{2\alpha\beta}}{|\hat{\psi}_2|} v_{1dq}^* \quad (4)$$

where the variables and the parameters are defined as below:

- v_1 : primary voltage vector
- i_1 : primary current vector
- ψ_2 : secondary flux vector
- T : output torque
- ω : rotating speed of the $d-q$ coordinates
- ω_m : rotating speed of the rotor
- R_1 : primary resistance
- R_2 : secondary resistance
- L_{11} : primary self inductance
- L_{22} : secondary self inductance
- M : mutual inductance
- $\ell = \frac{L_{11}L_{22} - M^2}{L_{22}}$: leakage inductance
- $\tau_2 = L_{22}/R_2$: secondary time constant
- p : differential operator
- j : imaginary unit
- \hat{x} : estimated value of x
- x^* : command of x
- $|x|$: amplitude of x
- $\text{Im}(x)$: imaginary part of x
- \bar{x} : complex conjugate of x
- $x_{\alpha\beta}$: vector x on the stator ($\alpha-\beta$) coordinates
- x_{dq} : vector x on the flux ($d-q$) coordinates

The simulator is called a rotor current model, which requires detecting the primary currents and the rotating speed of the rotor. The model can calculate the flux all over the speed range including zero speed because it does not possess pure integrators. On the $d-q$ coordinates rotating synchronously with ψ_{2dq} , the flux amplitude and the output torque can be controlled by manipulating the flux component i_{1d} and the torque component i_{1q} respectively. As it is necessary to control each component of the current, detected currents and voltage commands are transformed by using $\hat{\psi}_{2\alpha\beta}$ which is estimated in the flux simulator. Therefore, if the simulator estimates $\hat{\psi}_{2\alpha\beta}$ with an error, current control on the $d-q$ coordinates can not be carried out perfectly. This prevents the system from controlling the flux and the output torque without transient phenomena. The parameter mismatches of \hat{M} and $\hat{\tau}_2$ cause the estimation error. The former is caused by magnetic saturation (non-linearity), while the latter is caused by magnetic saturation and thermal variation. Figure 2 shows an example of inductances which were measured for a tested induction motor. It is found that ℓ is almost constant, but M varies widely according to the operating conditions.

Principle of Robust Identification of the Parameters

Identification of Leakage Inductance

It is possible to identify the mutual inductance and the secondary time constant assuming no parameter mismatch of the leakage inductance as described in the next section. In order to achieve more perfect on-line parameter tuning, the identification

of the leakage inductance, which is not affected by any other parameters, ought to be considered.

The equivalent circuit of the induction motor in the steady-state is given as shown in Fig. 3(a), which is for a fundamental angular frequency ω . For much higher angular frequency $\omega_h \gg \omega$, however, the circuit can be simplified as shown in Fig. (b). Therefore, the effects of M and ω_m can be neglected for the most part. It is assumed that the harmonic current vector i_{1h} is obtained according to the harmonic voltage vector v_{1h} . v_{1h} has an angular frequency ω_h and is superposed on the primary voltage vector command v_{1dq}^* in Fig. 1. The instantaneous harmonic reactive power Q_h is given by Eq. (5).

$$Q_h = \text{Im}(v_{1h}\bar{i}_{1h}) \quad (5)$$

On the other hand, the circuit equation for harmonics can be expressed as follows:

$$v_{1h} = (R_1 + R_2 + p\ell)i_{1h} \quad (6)$$

Substituting this equation into Eq. (5), the terms of R_1 and R_2 in Eq. (6) are canceled out perfectly, and the following equation is derived.

$$Q_h = \ell \text{Im}(p i_{1h}\bar{i}_{1h}) \quad (7)$$

Equations (5) and (7) have no parameter sensitivities to both R_1

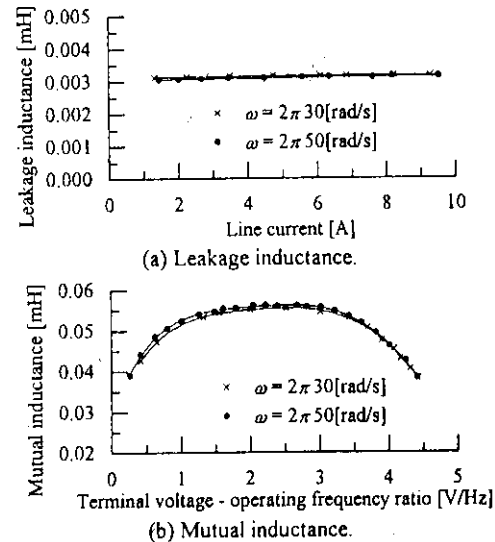


Fig. 2 Inductance of tested induction motor.

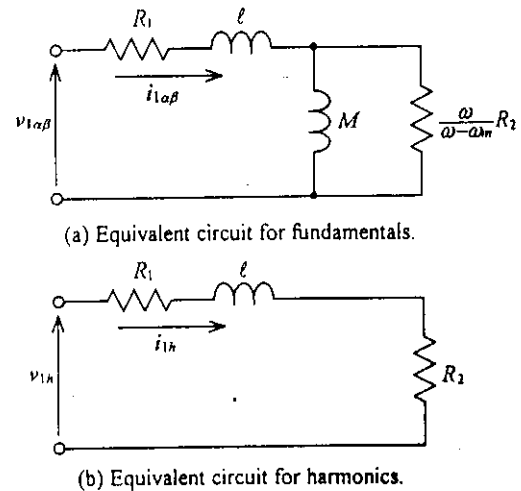


Fig. 3 Equivalent circuits of induction motor.

and R_2 , while Eq. (7) requires the value of the leakage inductance. If there is a parameter mismatch of it, Eq. (7) has an error; hence it is feasible to replace Eq. (7) with Eq. (8).

$$\hat{Q}_h = \hat{\ell} \text{Im}(p i_{1h} \bar{i}_{1h}) \quad (8)$$

The error between Eq. (7) which represents a true value and Eq. (8) can be calculated in the steady-state as follows:

$$\Delta Q_h = \omega (\ell - \hat{\ell}) |I_{1h}|^2 \quad (9)$$

Since $\omega \neq 0$, it is found that $\Delta Q_h = 0$ if and only if $\hat{\ell} = \ell$ from this equation. Therefore, it is possible to identify the leakage inductance value uniquely by using ΔQ_h in any conditions. As v_{1h} is a high frequency vector, winding resistance value increases more because of its skin effect. By using the instantaneous harmonic reactive power, however, the effect can be neglected, which is also an advantage of the proposed technique.

Figure 4 shows a configuration of the leakage inductance identifier. Q_h calculated by Eq. (5) is a reference model, and \hat{Q}_h estimated by Eq. (8) is a mathematical model. The error ΔQ_h adjusts dynamically $\hat{\ell}$ in Eq. (8). Identified value is also used for the identifier of the mutual inductance and the secondary time constant as described in the next section. It is important to extract i_{1h} from the primary current as precisely as possible. A digital filter can be used for this purpose, and it has a following transfer function.

$$H(z) = \frac{b_1(z^{-1} - z^{-2})}{1 - a_1 z^{-1} + a_2 z^{-2}} \quad (10)$$

Equation (10) gives a band-pass characteristics, and each coefficient is determined by its central frequency, quality factor and gain.

Identification of Mutual Inductance and Secondary Time Constant

In what follows, the identification technique of the mutual inductance and the secondary time constant, which is never affected by the variation of the primary resistance, is discussed.

The conventional technique is based on comparison between a stator voltage model and a rotor current model of the induction motor. It compensates for the parameters used in the rotor current model according to the output error of the two models. The error is calculated by Eq. (1) and Eq. (11) which is the stator voltage model.

$$\psi_{2\alpha\beta} = \frac{1}{p} (v_{1\alpha\beta} - R_1 i_{1\alpha\beta}) - \ell i_{1\alpha\beta} \quad (11)$$

This equation operates as a reference model, however it requires not only R_1 but also pure integrator. Consequently, the identification of the \hat{M} and $\hat{\tau}_2$ in Eq. (1) becomes imperfect because the integrator accumulates the error of R_1 . In order to avoid the above problem, the instantaneous reactive power of the induction motor Q is introduced.

Q is defined by the following equation on the α - β coordinates.

$$Q = \text{Im}(v_{1\alpha\beta} \bar{i}_{1\alpha\beta}) \quad (12)$$

This quantity is a scalar which is calculated statically by using the detected primary voltages and currents, which means that Eq. (12) does not require any integrator. It always gives a true value because no parameters of the induction motor are used. On the other hand, substituting $v_{1\alpha\beta}$ of Eq. (11) into Eq. (12), Q can be rewritten as follows:

$$Q = \text{Im}(p \psi_{2\alpha\beta} \bar{i}_{1\alpha\beta} + \ell p i_{1\alpha\beta} \bar{i}_{1\alpha\beta}) \quad (13)$$

The term of R_1 in Eq. (11) is canceled out perfectly in this derivation.⁴⁴ Therefore, Eq. (13) has no parameter sensitivity to

R_1 . Equation (13) requires $\psi_{2\alpha\beta}$, which may be calculated in the flux simulator. The simulator, however, uses the values of the mutual inductance and the secondary time constant as described before. Equation (13) possibly has an error owing to the parameter mismatches; hence it is feasible to replace Eq. (13) with Eq. (14).

$$\hat{Q} = \text{Im}(p \hat{\psi}_{2\alpha\beta} \bar{i}_{1\alpha\beta} + \hat{\ell} p i_{1\alpha\beta} \bar{i}_{1\alpha\beta}) \quad (14)$$

The difference between Eq. (13) and Eq. (14) can be derived as follows:

$$\Delta Q = \text{Im}\{p(\psi_{2\alpha\beta} - \hat{\psi}_{2\alpha\beta}) \bar{i}_{1\alpha\beta} + (\ell - \hat{\ell})(p i_{1\alpha\beta} \bar{i}_{1\alpha\beta})\} \quad (15)$$

The variations of the parameters are considerably slow compared with electrical time constants. Therefore it is enough to consider a steady-state, and the instantaneous variables can be replaced as $p \rightarrow j\omega$, $\psi_{2\alpha\beta} \rightarrow \Psi_2$, $\hat{\psi}_{2\alpha\beta} \rightarrow \hat{\Psi}_2$ and $i_{1\alpha\beta} \rightarrow I_1$ in Eq. (1) and Eq. (15), where the upper-case variables represent phasors in the steady-state. Then ΔQ is calculated as follows:

$$\Delta Q = \omega \left[\frac{M - \hat{M} + (\omega - \omega_m)^2 (M \hat{\tau}_2^2 - \hat{M} \tau_2^2)}{\{1 + (\omega - \omega_m)^2 \tau_2^2\} \{1 + (\omega - \omega_m)^2 \hat{\tau}_2^2\}} + \ell - \hat{\ell} \right] |I_1|^2 \quad (16)$$

It is recognized that there are infinitely many solutions which can make ΔQ zero from this equation; hence each parameter can not be identified uniquely without any restrictions. Assuming no load condition and that $\hat{\ell}$ has converged to a true value (This identification technique was discussed in the previous section),

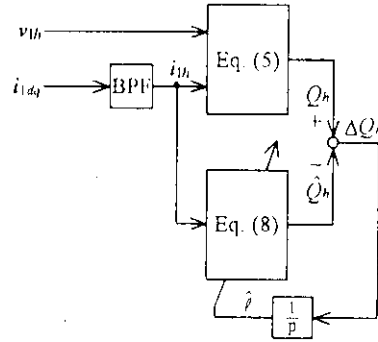


Fig. 4 Leakage inductance identifier.

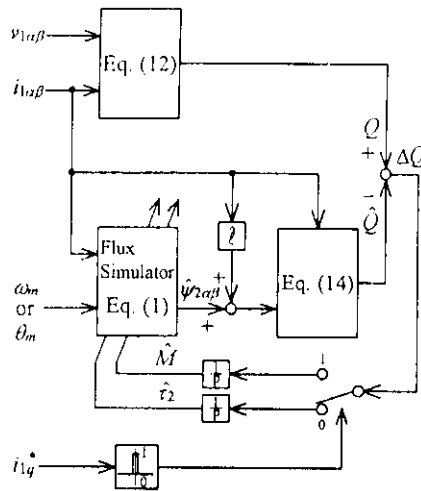


Fig. 5 Mutual inductance and secondary time constant identifier.

Eq. (16) is simplified as follows:

$$\Delta Q = \omega(M - \hat{M})|I_1|^2 \quad (17)$$

It is found that $\Delta Q = 0$ if and only if $\hat{M} = M$ except the case of $\omega = 0$ from this equation. In other words, it is possible to identify the mutual inductance value uniquely by using ΔQ in the no load condition. Assuming that the identification of M has finished on the basis of the above process, that is $\hat{M} = M$, Eq. (16) can be rewritten as follows:

$$\Delta Q = \frac{\omega(\omega - \omega_m)^2 M(\hat{\tau}_2 - \tau_2)(\hat{\tau}_2 + \tau_2)}{\left\{1 + (\omega - \omega_m)^2 \hat{\tau}_2^2\right\} \left\{1 + (\omega - \omega_m)^2 \tau_2^2\right\}} |I_1|^2 \quad (18)$$

It is found that $\Delta Q = 0$ if and only if $\hat{\tau}_2 = \tau_2$ except the case of $\omega = 0$ or $\omega = \omega_m$ from this equation. Therefore, it is possible to identify the secondary time constant value uniquely by using ΔQ except the condition of no load.

Figure 5 shows a block diagram of the mutual inductance and the secondary time constant identifier, which is robust against the variation of the primary resistance. The identifier is

based on a parallel-type model reference adaptive system. Q of Eq. (12) is a process, and the flux simulator and \hat{Q} of Eq. (14) constitutes a mathematical model. The error ΔQ is used to adjust \hat{M} and $\hat{\tau}_2$ in the flux simulator dynamically. Two integrators are employed as identification algorithms because of slow variations of the parameters as mentioned before. They are switched complementarily by using torque component current command i_{1q}^* . Identification algorithm of \hat{M} is selected under the no load condition, and that of $\hat{\tau}_2$ is selected under the loaded condition. If the case of $\omega = 0$ or $\omega = \omega_m$ occurs, the identification algorithms hold the values which have been integrated as \hat{M} and $\hat{\tau}_2$, and they do not diverge.

Digital Simulation and Results

A digital simulation was conducted on the control system described above. Robustness against the primary resistance and adaptability to the leakage inductance, the mutual inductance and the secondary time constant were examined through the

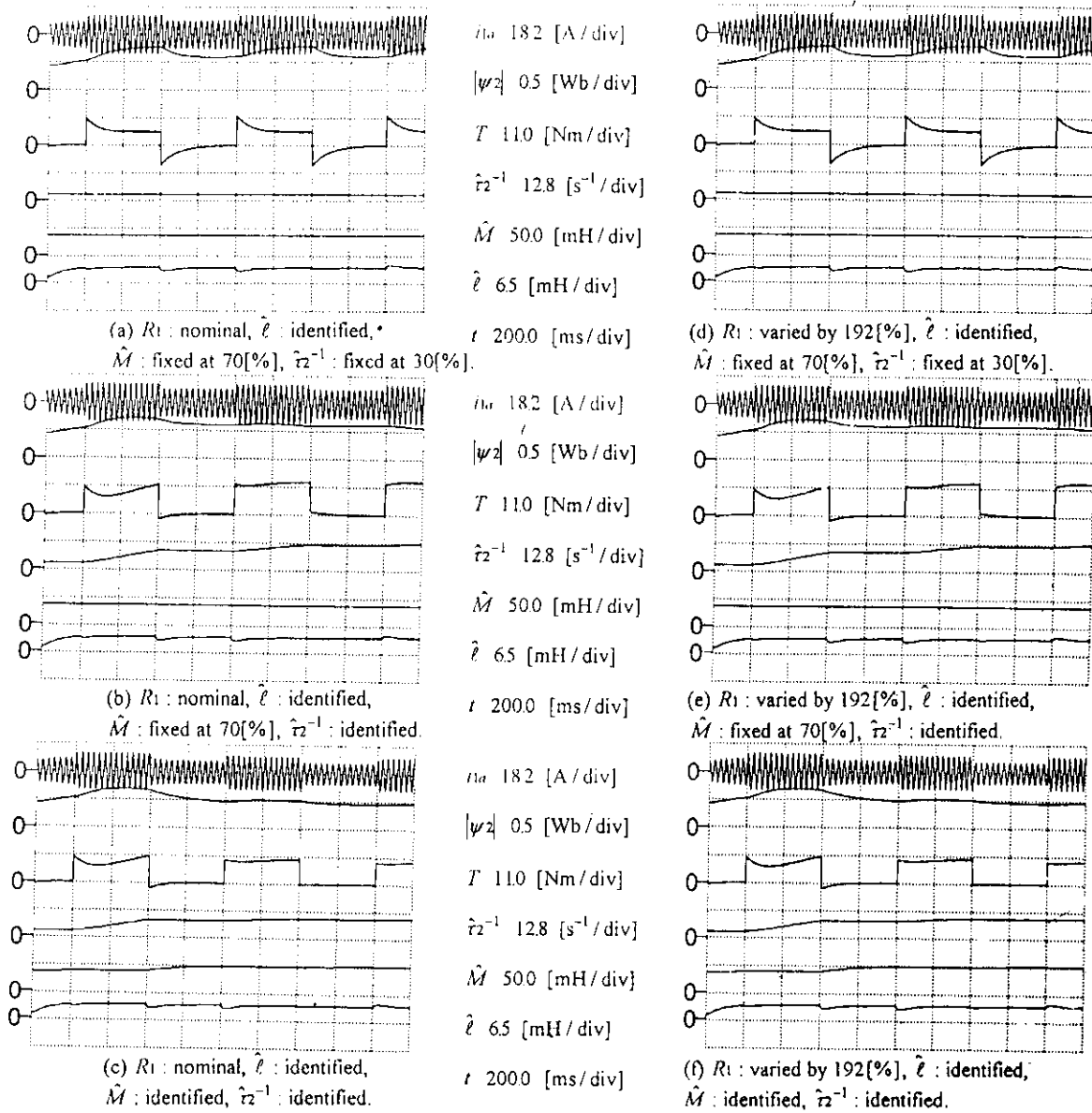


Fig. 6 Characteristics of parameter identification and torque control (simulation results).

simulations. The parameters of the induction motor are shown in Table 1, and its output torque was controlled under the condition of a constant rotating speed. The harmonic voltage vector and the digital filter used in the leakage inductance identifier are shown below.

$$v_{1h} = 8.0e^{j2\pi 303.5t} \quad (19)$$

$$a_1 = 1.9782, a_2 = 0.9878, b_1 = 0.0974 \quad (20)$$

central frequency : 303.5[Hz]

quality factor : 8.0

gain : 8.0

Figure 6 shows step torque responses of 100[%] torque command, and the command is changed intermittently at low frequency (1.25[Hz]). Condition of each simulation is described in its caption. Leakage inductance is identified simultaneously in every case. As shown in every figure, identification of $\hat{\ell}$ is performed in about 200[ms], and is found to be robust against any other parameters. Small deviations of identified inductance are observed when the output torque steps up and down, which is owing to the transient characteristics of the digital filter. Comparing Figs. (a) ~ (c) with Figs. (d) ~ (f), it is found that the proposed method is robust against the variation of R_1 . Because field-oriented control system has a current control loop, and proposed technique is based on the identifiers using instantaneous reactive power. The parameter mismatches of \hat{M}

and $\hat{\tau}_2$ in the flux simulator cause transient phenomena in both flux and torque responses. Figures 6(a) and (d) show degradation of the responses. The parameter mismatches of

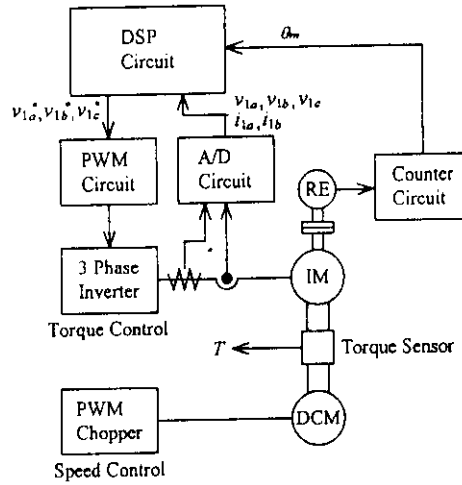
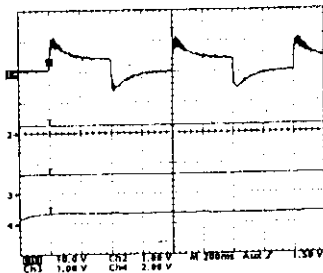
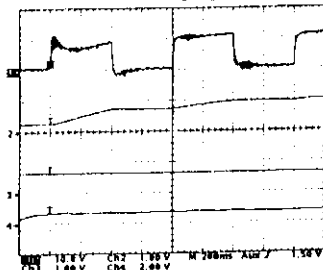


Fig. 7 Experimental system.



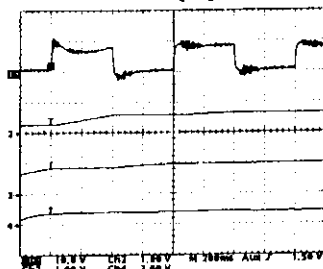
(a) R_1 : nominal, $\hat{\ell}$: identified, \hat{M} : fixed at 70[%], $\hat{\tau}_2^{-1}$: fixed at 30[%].

T 110 [Nm/div]
 $\hat{\tau}_2^{-1}$ 12.8 [s^{-1} /div]
 \hat{M} 50.0 [mH/div]
 $\hat{\ell}$ 6.5 [mH/div]
 t 200.0 [ms/div]



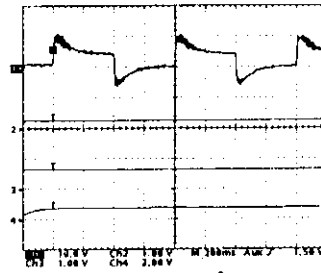
(b) R_1 : nominal, $\hat{\ell}$: identified, \hat{M} : fixed at 70[%], $\hat{\tau}_2^{-1}$: identified.

T 110 [Nm/div]
 $\hat{\tau}_2^{-1}$ 12.8 [s^{-1} /div]
 \hat{M} 50.0 [mH/div]
 $\hat{\ell}$ 6.5 [mH/div]
 t 200.0 [ms/div]

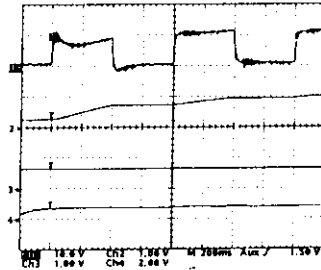


(c) R_1 : nominal, $\hat{\ell}$: identified, \hat{M} : identified, $\hat{\tau}_2^{-1}$: identified.

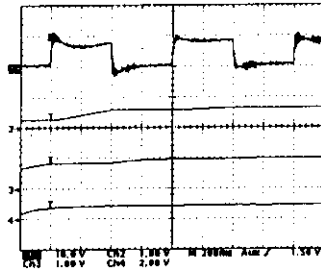
T 110 [Nm/div]
 $\hat{\tau}_2^{-1}$ 12.8 [s^{-1} /div]
 \hat{M} 50.0 [mH/div]
 $\hat{\ell}$ 6.5 [mH/div]
 t 200.0 [ms/div]



(d) R_1 : varied by 192[%], $\hat{\ell}$: identified, \hat{M} : fixed at 70[%], $\hat{\tau}_2^{-1}$: fixed at 30[%].



(e) R_1 : varied by 192[%], $\hat{\ell}$: identified, \hat{M} : fixed at 70[%], $\hat{\tau}_2^{-1}$: identified.



(f) R_1 : varied by 192[%], $\hat{\ell}$: identified, \hat{M} : identified, $\hat{\tau}_2^{-1}$: identified.

Fig. 8 Characteristics of parameter identification and torque control (experimental results).

them ought to be compensated without any relations with R_1 to improve the responses. On the other hand, if only $\hat{\tau}_2$ is identified with parameter mismatch of \hat{M} as shown in Figs. (b) and (e), its identification characteristics are degraded. The reason of this degradation is that unique convergence of $\hat{\tau}_2$ can not be certified under the condition of parameter mismatch of \hat{M} in Eq. (16). Transient phenomena are remained in the responses of flux and torque. When both \hat{M} and $\hat{\tau}_2$ are identified as shown in Figs. (c) and (f), however, the flux and torque responses are improved successfully with their convergence to the true values. A quick torque response was obtained without any transient oscillation and steady-state errors.

Experimental System and Results

Outline of Experimental System

Some experimental tests were carried out to confirm the feasibility of the proposed scheme. Figure 7 shows a schematic diagram of an experimental system. The system consists of an inverter fed induction motor and a chopper fed dc motor. The parameters of the induction motor are as same as those shown in Table 1.

A fully digitized software control system was developed for the induction motor. The control and identification process is completely based on DSP (TMS320C50, 1 instruction cycle : 50[ns]) software, and the control program is proceeded in 103.0[μ s] for every control period, while the program concerning the leakage inductance identifier which deals with a higher frequency is performed in every 51.5[μ s]. Specifications of the harmonic voltage vector and the digital filter are as same as described in Eqs. (19) and (20). The output torque of the induction motor is controlled by the system without a speed loop.

A load of the induction motor is the dc motor system which has both current and speed loops to keep the mechanical rotating speed constant. The shafts of the two motors are coupled with a distortion-gage-type torque pickup. The actual output torque of the induction motor can be observed with it.

Experimental Results

Figures 8(a) ~ (f) show experimental results of the above system. The experiments were conducted under the same conditions as those of simulations. The primary resistance was varied by inserting the external resistors of 0.5[Ω]. As shown in every figure, $\hat{\ell}$ is identified without any effects of other parameters as well as simulation results. In addition to that, the characteristics of the torque response and the identification are found to be robust comparing Figs. (a) ~ (c) with Figs. (d) ~ (f).

As shown in Figs. (a) and (d), transient phenomena were measured in the torque responses because of the parameter mismatches of \hat{M} and $\hat{\tau}_2$. The output torque was decreased by 50[%] in the steady-state. On the other hand, improvement of the torque response was confirmed by Figs. (c) and (f). Transient phenomena in the responses were observed at the beginning of the identifications because there were parameter mismatches in their initial values. However, the identification started automatically, and each of \hat{M} and $\hat{\tau}_2$ converged to a certain constant value. The value of $\hat{\tau}_2$ in this experimental case was rather smaller than the nominal value. It is supposed that the nominal value included nearly 20[%] errors because it had been determined by using L-type equivalent circuit with thermal conversion. Then the torque responses were improved successfully without any transient oscillations and steady-state

errors. The torque response time was about 3[ms], and this performance was almost as same as dc motor. In addition to that, the variation of R_1 did not affect the compensation process as shown in Fig. (d).

Conclusions

The authors proposed a torque control strategy of an induction motor with robustness against the variations of the primary resistance and adaptability to the leakage inductance, the mutual inductance and the secondary time constant. In this paper, several results were obtained through the theoretical consideration, some digital simulations and experimental tests. The flux-feedback-type field-oriented control is essentially robust against the variation of the primary resistance because its flux simulator employs a rotor current model. The variations of the mutual inductance and the secondary time constant, however, affect strongly the control performance. Introducing a robust identifier, their variations can be compensated completely without any effects of the primary resistance. The identifier is based on the instantaneous reactive power of the induction motor, and it can identify the mutual inductance and the secondary time constant automatically and uniquely. Moreover, this paper described a leakage inductance identification technique, which is based on the instantaneous harmonic reactive power of the induction motor. The techniques proposed by the authors are supposed to make induction motor drives perfectly free from adjustments of their parameters.

References

- [1] C. Wang, D. W. Novotny and T. A. Lipo, "An Automated Rotor Time Constant Measurement System for Indirect Field-Oriented Drives," *IEEE Trans. on Ind. App.*, IA-24, 151-159, 1988
- [2] A. Gastli, M. Iwasaki and N. Matsui, "An Automated Equivalent Circuit Parameter Measurements of an Induction Motor Using V/F PWM Inverter," *IPEC-Tokyo Conf. Rec.*, 659-666, 1990
- [3] M. Akiyama, K. Kobayashi, I. Miki and M. A. El-sharkawi, "Auto-Tuning Method for Vector Controlled Induction Motor Drives," *IPEC-Yokohama Conf. Rec.*, 789-794, 1995
- [4] J. Holtz and T. Thimm, "Identification of the Machine Parameters in a Vector Controlled Induction Motor Drive," *IEEE IAS Ann. Meet. Conf. Rec.*, 601-606, 1989
- [5] J. Moreira, K. Hung, T. Lipo and R. Lorenz, "A Simple and Robust Adaptive Controller for Detuning Correction in Field Oriented Induction Machines," *IEEE IAS Ann. Meet. Conf. Rec.*, 397-403, 1991
- [6] L. J. Garcés, "Parameter Adaption for the Speed-Controlled Static AC Drive with a Squirrel-Cage Induction Motor," *IEEE Trans. on Ind. App.*, IA-16, 173-178, 1980
- [7] K. Tungpimolrut, F. Peng and T. Fukao, "Robust Vector Control of Induction Motor without Using Stator and Rotor Circuit Time Constants," *IEEE IAS Ann. Meet. Conf. Rec.*, 521-527, 1993
- [8] T. Noguchi, S. Kondo and I. Takahashi, "Robust Torque Control of Induction Motor against Variations of Primary and Secondary Resistances," *IPEC-Tokyo Conf. Rec.*, 1163-1168, 1995

Table 1. Nominal parameters and rated values of tested motor.

Rated output	1.5[kW]	ℓ	3.1[mH]
Rated torque	8.63[Nm]	M	51.0[mH]
R_1	0.542[Ω]	$ \psi_2 $	0.427[Wb]
R_2	0.536[Ω]	ω_m	104.7[rad/s]